A Tale of Three LPAs: Some Notes on Zig-Zag Log-Periodic Arrays
3. The X or Saw Tooth Zig-Zag LPA

L. B. Cebik, W4RNL

The trapezoid was not the only solid-surface element shape to have a wire-outline analog in the development of LPAs. Performing similarly to the trapezoid was the saw tooth shape, shown in wire-outline single-bay form in **Fig. 1**. Like the trapezoid, solid-surface forms used a central boom composed of a line that grew wider as the distance from the vertex increased. The wire-outline version reduced the central line to the diameter of the wire itself. Folding two bays together produced a directional beam. From above, the pattern of elements formed the series of Xs that yields the casual array name.

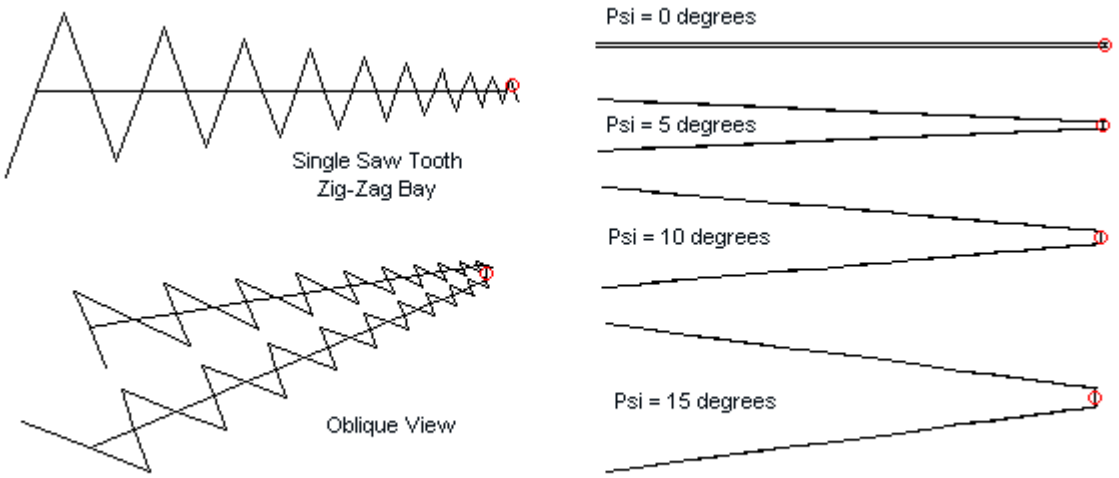

General Outlines of X (Saw Tooth) Zig-Zag LPAs with Booms

Fig. 1

In the early 1960s, J. W. Carr discovered that he could remove the central boom and still have a useful beam. Therefore, we shall have to see whether boomless X LPAs are more or less successful than boomless trapezoidal arrays. Finally, we shall look at two amateur examples of X LPAs using far less stringent design criteria than the ones we shall employ in our main comparative study.

As we did for the LPDA and the trapezoidal zig-zag array, we shall impose design parameters that best assure us of reasonable performance. Even though the arrays are too long to be practical for most cases, they serve modeling needs well. When $\tau = 0.9$, $\sigma = o.167$, and $\alpha' = 17°$, we obtain worthwhile performance over all or most of the 50-200 MHz operating passband. The ψ-angle will be subject to variation to explore any differences that it makes to performance. The limits of NEC modeling dictate that we use rather thin wire, in this case, 0.1" (2.54-mm) lossless wire for all elements. Each bay will use 20 elements, resulting in fairly sizable models. As a review, **Fig. 2** provides the spreadsheet page that indicates the dimensions used in the models.

The zig-zag X LPA handles the dimensions in a slightly different manner than did the LPDA and the trapezoidal arrays. If we think of a Cartesian axis as the centerline of the model, the earlier LPAs defined each element as extending for Ln/2 on both sides of the centerline. The saw tooth zig-zag alters the arrangement such that the first element extends from –L1/2 to

+L2/2. In the process, it also moves forward toward the vertex from R1 to R2. The next element reverses and increments the process.

Zig-Zag Log-Periodic Antenna Elements											Fig. 2
Work Sheet		**Bold = User Entry**									
Tau		**0.90**								Sigma	0.167
Alpha'	degrees	**17.00**	degrees	0.297	radians	1/2Alpha'	0.148	tanAlpha	0.1495		0.167
F-low		**50.00**	MHz								
F-high		**200.00**	MHz								
L-long		3.00	meters	9.84	feet	118.11	inches				
Lhigh		0.75	meters	2.46	feet	29.53	inches				
L*1.6		0.47	meters	1.54	feet	18.45	inches				
Rv	Vertex R	10.04	meters	32.93	feet	395.15	inches				
Element	Ln	Ln/2	Rn	Element	Lfeet	Lft/2	Rfeet	Element	Linch	Lin/2	Rinch
1	3.00	1.50	10.04	*1*	9.84	4.92	32.93	*1*	118.11	59.06	395.15
2	2.70	1.35	9.03	*2*	8.86	4.43	29.64	*2*	106.30	53.15	355.63
3	2.43	1.22	8.13	*3*	7.97	3.99	26.67	*3*	95.67	47.83	320.07
4	2.19	1.09	7.32	*4*	7.18	3.59	24.01	*4*	86.10	43.05	288.06
5	1.97	0.98	6.59	*5*	6.46	3.23	21.60	*5*	77.49	38.75	259.26
6	1.77	0.89	5.93	*6*	5.81	2.91	19.44	*6*	69.74	34.87	233.33
7	1.59	0.80	5.33	*7*	5.23	2.62	17.50	*7*	62.77	31.38	210.00
8	1.43	0.72	4.80	*8*	4.71	2.35	15.75	*8*	56.49	28.25	189.00
9	1.29	0.65	4.32	*9*	4.24	2.12	14.17	*9*	50.84	25.42	170.10
10	1.16	0.58	3.89	*10*	3.81	1.91	12.76	*10*	45.76	22.88	153.09
11	1.05	0.52	3.50	*11*	3.43	1.72	11.48	*11*	41.18	20.59	137.78
12	0.94	0.47	3.15	*12*	3.09	1.54	10.33	*12*	37.06	18.53	124.00
13	0.85	0.42	2.83	*13*	2.78	1.39	9.30	*13*	33.36	16.68	111.60
14	0.76	0.38	2.55	*14*	2.50	1.25	8.37	*14*	30.02	15.01	100.44
15	0.69	0.34	2.30	*15*	2.25	1.13	7.53	*15*	27.02	13.51	90.40
16	0.62	0.31	2.07	*16*	2.03	1.01	6.78	*16*	24.32	12.16	81.36
17	0.56	0.28	1.86	*17*	1.82	0.91	6.10	*17*	21.89	10.94	73.22
18	0.50	0.25	1.67	*18*	1.64	0.82	5.49	*18*	19.70	9.85	65.90
19	0.45	0.23	1.51	*19*	1.48	0.74	4.94	*19*	17.73	8.86	59.31
20	0.41	0.20	1.36	*20*	1.33	0.66	4.45	*20*	15.95	7.98	53.38

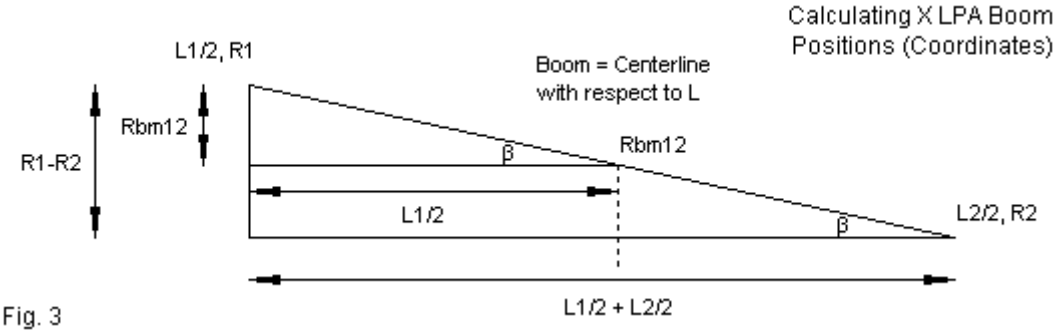

Fig. 3

Fig. 3 shows the first element along with a simple solution to the question of where to position the junction of the element with the boom at the array centerline. The position of Rbm12, the boom section that extended from element 1 to element 2, relative to the array vertex is proportional to the ratio of L1/2 to L1/2+L2/2. We may calculate the position of Rbm12 either from the proportionality of congruent triangles or by obtaining the tangent of the angle shown as β in the diagram. Once we have the position of the first boom junction, we may find all other junctions by multiply successively by the value of τ. **Fig. 4** provides the calculated values of Rbm for the X LPAs equipped with booms. The single-bay and the oblique double-bay diagrams in **Fig. 1** should suffice to confirm the accuracy of the method.

X-LPA Boom Calculations			Fig. 4
Adjacent	2.85		
Opposite	1.003673		
tanBeta	0.352166		
Rbm-n	9.508485		
Boom	Rbm-m	Rbm-ft	Rbm-in
1-2	9.508	31.20	374.35
2-3	8.558	28.08	336.91
3-4	7.702	25.27	303.22
4-5	6.932	22.74	272.90
5-6	6.239	20.47	245.61
6-7	5.615	18.42	221.05
7-8	5.053	16.58	198.94
8-9	4.548	14.92	179.05
9-10	4.093	13.43	161.15
10-11	3.684	12.09	145.03
11-12	3.315	10.88	130.53
12-13	2.984	9.79	117.47
13-14	2.685	8.81	105.73
14-15	2.417	7.93	95.15
15-16	2.175	7.14	85.64
16-17	1.958	6.42	77.08
17-18	1.762	5.78	69.37
18-19	1.586	5.20	62.43
19-20	1.427	4.68	56.19
20-21	1.284	4.21	50.57

As with earlier double-bay models, we shall not try to extend forward leads all the way to the vertex. As **Fig. 4** indicates, the distance from the forward-most element to the vertex is several times longer than the distance between elements. Directly connecting the booms with a single direct lead provides the most economical model with no harmful effects on the reported data.

X LPAs with Booms.

X or saw tooth LPAs equipped with central booms have current magnitude distribution curves that are as difficult to decipher as their trapezoidal counterparts. **Fig. 5** shows the distribution curve set for one of the LPAs at 50 MHz. In the side view of the array, the nearly level lines represent currents on the boom, while the more curved lines represent currents on the angular elements. The face view of the array's upper bay shows only the element currents.

Although more difficult to see due to the angularity of the elements, the boom-equipped X LPA preserves some, if not most, of the properties associated with the solid-surface bay that the wire-outline version approximates. Current magnitude may abruptly change as an element intersects the boom, since the currents on each side are associated with a different saw-tooth shape. In the side view, the most active region in terms of peak current magnitude for the X LPA extends for a considerable distance toward the vertex. However, the element angles and the disparate collection of wire sections involved do not allow us to see fine detail.

Fig. 1 shows the range of ψ-angles that we shall examine for X LPAs with booms. The data will clarify why I limited the range to 0° to 20° in 5° increments. We may sample the performance at each ψ-angle using the data in **Table 1**, which provides values for 50, 100, 150, and 200 MHz.

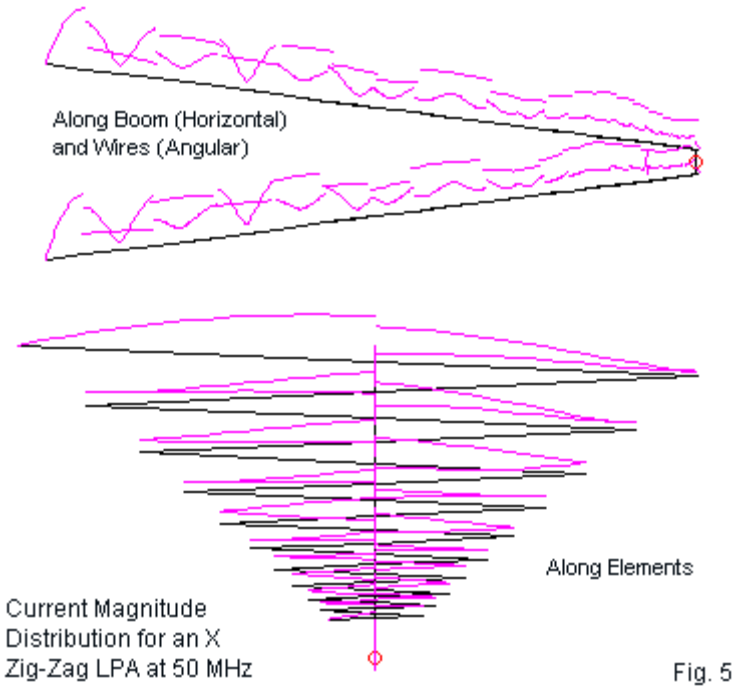

Fig. 5

Table 1. Sample performance values of X zig-zag LPAs using various ψ-angles

1. 20 elements/bay, α = 17°, τ = 0.9, ψ = 0° (flat array, 4" separation between bays)

Frequency MHz	Max. Gain dBi	Front-Back Ratio dB	E BW degrees	H BW degrees	Impedance R +/- jX Ω	250-Ω SWR
50	7.28	15.70	64.2	99.2	276 - j 26	1.15
100	8.13	30.62	64.6	95.6	270 - j 33	1.16
150	8.29	27.14	64.2	94.6	246 - j 23	1.10
200	8.43	22.34	63.0	91.8	178 - j 12	1.41

2. 20 elements/bay, α = 17°, τ = 0.9, ψ = 5°

Frequency MHz	Max. Gain dBi	Front-Back Ratio dB	E BW degrees	H BW degrees	Impedance R +/- jX Ω	250-Ω SWR
50	7.64	11.96	63.5	90.2	252 - j 78	1.36
100	8.64	29.77	63.8	88.0	267 - j 39	1.18
150	8.70	26.57	64.0	88.8	241 - j 20	1.09
200	8.79	22.60	62.4	86.8	175 - j 7	1.44

3. 20 elements/bay, α = 17°, τ = 0.9, ψ = 10°

Frequency MHz	Max. Gain dBi	Front-Back Ratio dB	E BW degrees	H BW degrees	Impedance R +/- jX Ω	300-Ω SWR
50	8.25	9.06	62.8	77.0	324 – j138	1.56
100	9.38	23.42	64.0	76.3	307 - j 1	1.02
150	9.44	22.14	63.4	75.6	268 +j 44	1.21
200	9.27	18.23	63.0	75.8	197 + j 93	1.75

4. 20 elements/bay, α = 17°, τ = 0.9, ψ = 15°

Frequency MHz	Max. Gain dBi	Front-Back Ratio dB	E BW degrees	H BW degrees	Impedance R +/- jX Ω	300-Ω SWR
50	8.72	6.87	63.0	63.1	368 – j185	1.79
100	9.52	18.88	68.0	64.6	381 + j 38	1.30
150	9.65	18.81	65.8	63.2	303 + j 94	1.36
200	9.48	15.81	62.4	62.0	230 + j202	2.21

As we increase the value of ψ, the reference impedance for general SWR values increases from 250 Ω to 300 Ω. One of the two major limiting factors in X LPA performance is the rising reactance value as the ψ-angle increases, resulting in SWR values that exceed the normal 2:1 limit that we often employ as a standard. The other limitation is the gain and front-to-back performance at the low end of the passband. The rising gain value at 50 MHz does not keep pace with the rapidly declining front-to-back value at that frequency. We may re-affirm these general impressions using summary frequency sweep data, shown in **Table 2**.

Table 2. Frequency sweep summery of X zig-zag LPAs using various ψ-angles from 50 to 200 MHz

1. ψ = 0°

Category	Minimum	Maximum	Δ	Average
Gain dBi	7.28	8.44	1.16	8.17
Front-Back dB	15.70	34.21	18.51	27.84
E Beamwidth °	63.0	65.5	2.5	64.3

2. ψ = 5°

Category	Minimum	Maximum	Δ	Average
Gain dBi	7.64	8.84	1.20	8.64
Front-Back dB	11.96	30.93	18.97	26.87
E Beamwidth °	62.4	64.6	2.2*	63.5

*Least variation across the passband of the group.

3. ψ = 10°

Category	Minimum	Maximum	Δ	Average
Gain dBi	8.25	9.52	1.27	9.31
Front-Back dB	9.06	25.85	17.69	21.75
E Beamwidth °	62.6	65.4	2.8	63.8

4. ψ = 15°

Category	Minimum	Maximum	Δ	Average
Gain dBi	8.72	9.87	1.15*	9.56
Front-Back dB	6.87	22.01	15.14	17.49
E Beamwidth °	62.1	69.8	7.7	65.5

*Least variation across the passband of the group.

Because the data with the smallest range of variation does not focus upon a single ψ-angle, my selection of a representative array for graphical presentation is somewhat arbitrary. I selected the version in which ψ = 5° for several reasons. The SWR remains below 2:1 across the operating range. The average front-to-back ratio has not begun its rapid decline. As well, the E-plane beamwidth shows the least variation across the operating range. Indeed, the patterns shown in **Fig. 6** display good control, allowing for the lesser performance of the X LPA

at the low end of the operating range. Any implementation of this array would naturally wish to begin with a longer rear element.

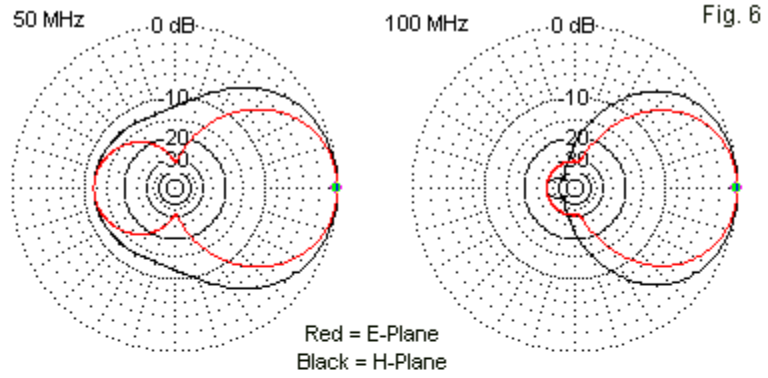

Fig. 6

20 Elements/Bay, Alpha = 17°, Tau = 0.9, Psi = 5°
Sample Free-Space E-Plane and H-plane Patterns

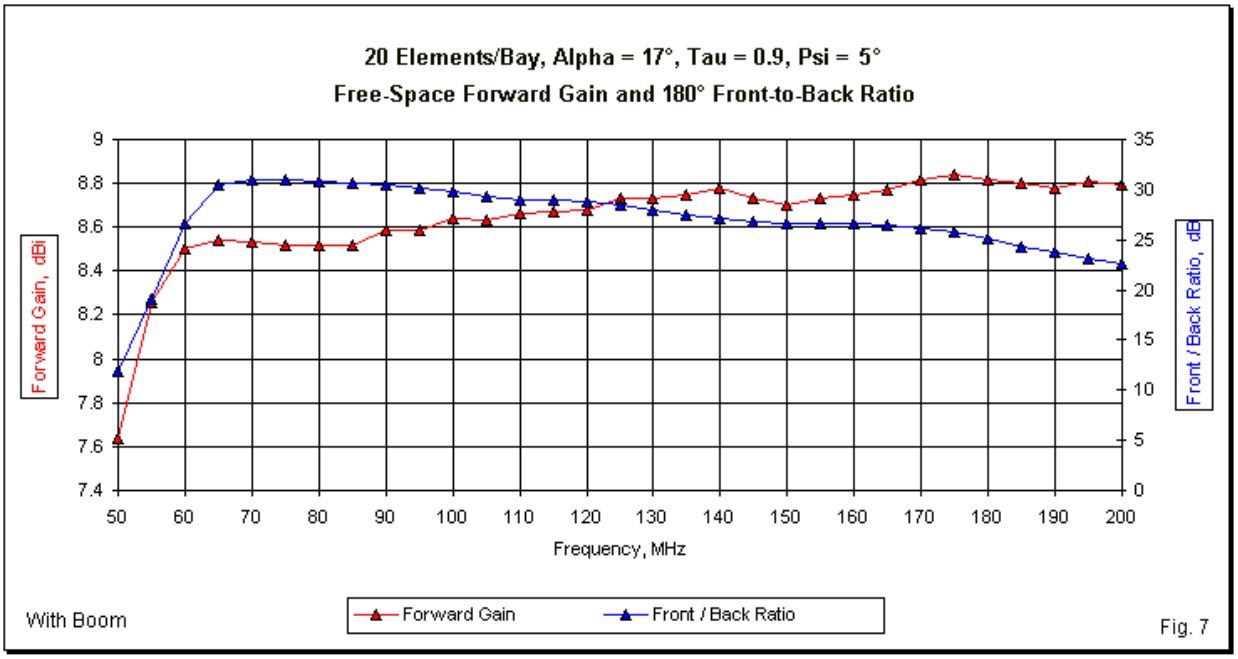

Fig. 7

The sweep graph of free-space forward gain and 180° front-to-back ratio confirms the general decline of performance below 60 MHz. Otherwise, the curves are exceptionally smooth. Equally smooth are the impedance curves (resistance, reactance, and 250-Ω SWR) shown in **Fig. 8**. Below 55 MHz, we can see a sudden turn in all of the values, although the sweep limits do not inform us of where the curves go below 50 MHz. Nevertheless, the combination of sweep performance graphs suggests that the span of good impedance performance is greater than the span of peak gain and front-to-back performance.

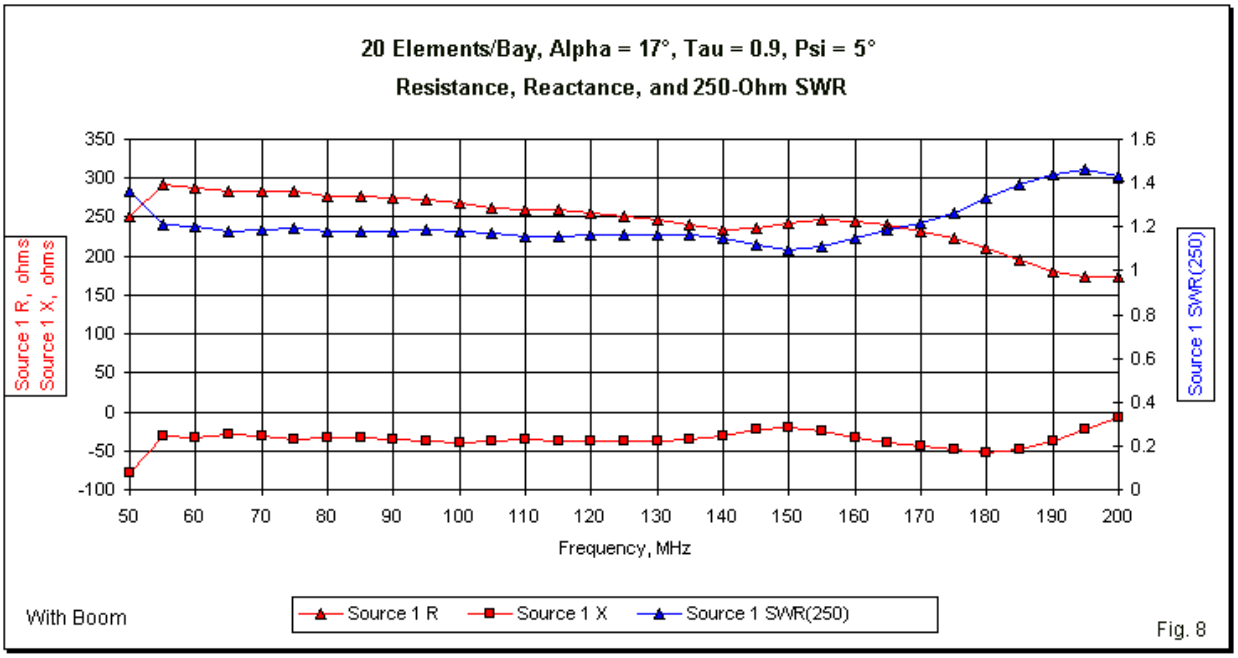

Fig. 8

Very little distinguishes the performance of boom-equipped trapezoidal LPAs and their X counterparts, once we compensate for any deficiencies at one or the other end of the operating passband. One might profitably study the corresponding data for all ψ-angles for both types of arrays in the data appendix.

X LPAs without Booms

Carr's innovation of removing the central boom from a zig-zag saw tooth bay resulted in a usable configuration. Unlike the boomless trapezoidal array, the boomless X array saw considerable use, especially in magazine plans for home-built television antennas. Therefore, we shall examine this type of array, using our standard design parameters, to see how it measures up against both the trapezoidal version and against the X LPA with a central boom.

The dimensions and design values are the same as used for the trapezoidal array and outlined in **Fig. 2**. $\tau = 0.9$ and $\alpha' = 17°$. The only difference is the omission of the side wires. Each element extends from a point defined by the limit of one element to the opposite limit determined by the value of τ applied to the initial limit. The result is two opposing bays of saw tooth elements that form a series of Xs when viewed directly from above or below. Like the trapezoidal array, the two bays have an angular separation determined by experimentally selected values of ψ. The models of the X LPAs created a wire connecting the free ends of the innermost elements on which to place the model source, since alternative lead arrangements created no significant changes in performance.

Because the X-version of the zig-zag LPA has no side wires, we may more easily see the current magnitude distribution along the wires. In **Fig. 9**, the blue dots represent wire ends and, therefore, changes in the wire direction. The green sections are the intervening wires as seen from the array side. The accompanying general outline of this model, which uses a ψ of 10°, provides an orientation to the wires from an oblique angle.

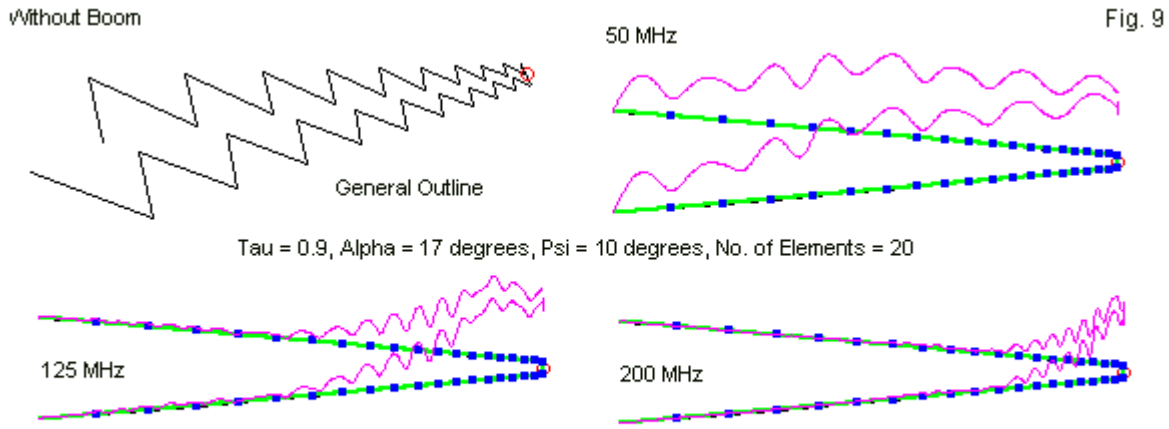

General Outline and Current Magnitude Distribution Along an X Zig-Zag Array at 3 Frequencies within the Operating Range

Like the trapezoidal zig-zag array, the X LPA shows the same tendency toward a maximum current peak along each bay that is far forward of the corresponding element on an LPDA. As well, the absence of wire free ends reveals that the current minimums do not necessarily occur at the points where the wire changes direction. See **Fig. 10**, which shows significant differences in the current curves relative to the version in **Fig. 5**. Note especially that some of the parallels to the current of solid-surface elements are missing.

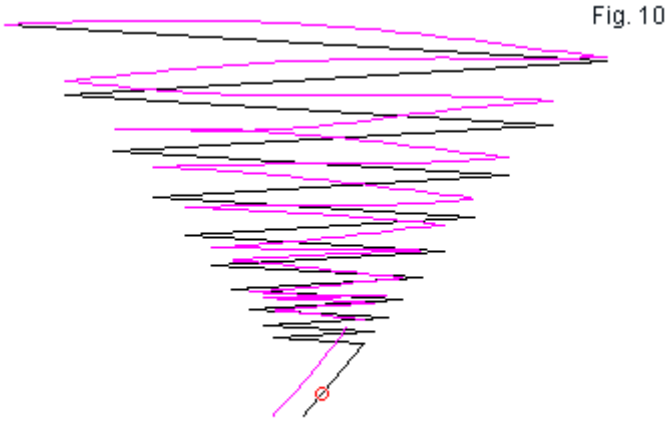

50-MHz Current Magnitude Distribution Along One Element Bay of an X Zig-Zag LPA

To allow more detailed comparisons between the trapezoidal and the X LPAs, we may look at sample data at 50, 100, 150, and 200 MHz for the range of ψ-angles covered by this initial exploration. The range of ψ-angles for the X LPA is not the same as for the trapezoidal counterpart. X arrays have been successfully used when ψ = 0°, with a small separation between the bays. In fact, we shall later discover that a ψ of 10° may be the most optimal angle

between bays when measured by the criteria used to select the optimal trapezoidal array. Therefore, the sample includes ψ-angles of 0°, 10°, 15°, and 20°. **Table 3** provides the results of the sampling.

Table 3. Sample performance values: X (saw tooth) array: 20 elements/bay, α = 17°, τ = 0.9

1. ψ = 0° (flat array, 4" separation between bays)

Frequency MHz	Max. Gain dBi	Front-Back Ratio dB	E BW degrees	H BW degrees	Impedance R +/- jX Ω	600-Ω SWR	500-Ω SWR
50	6.51	11.66	84.6	117.4	477 + j 61	1.29	1.14
100	6.34	12.15	87.4	115.2	446 + j 57	1.37	1.18
150	6.86	15.69	79.6	103.4	504 – j119	1.32	1.27
200	5.79	16.53	107.2	134.0	301 + j 18	2.00	1.67

2. ψ = 5°

Frequency MHz	Max. Gain dBi	Front-Back Ratio dB	E BW degrees	H BW degrees	Impedance R +/- jX Ω	600-Ω SWR
50	7.42	11.42	76.4	99.0	573 – j160	1.32
100	7.50	14.18	73.2	93.4	458 - j 98	1.39
150	6.95	16.78	77.2	98.8	577 - j 6	1.04
200	6.35	18.14	100.4	124.8	307 - j 15	1.96

3. ψ = 10°

Frequency MHz	Max. Gain dBi	Front-Back Ratio dB	E BW degrees	H BW degrees	Impedance R +/- jX Ω	600-Ω SWR
50	7.90	9.46	74.2	83.8	754 + j 78	1.29
100	7.32	18.82	82.4	91.4	619 - j 99	1.18
150	7.04	17.72	83.4	95.6	592 + j 82	1.15
200	7.21	16.69	90.2	96.6	332 - j 30	1.81

4. ψ = 15°

Frequency MHz	Max. Gain dBi	Front-Back Ratio dB	E BW degrees	H BW degrees	Impedance R +/- jX Ω	600-Ω SWR
50	8.34	7.53	73.4	69.0	726 + j 217	1.46
100	7.23	9.58	88.4	79.0	658 - j 87	1.18
150	7.27	13.34	89.6	79.6	672 + j 94	1.21
200	7.50	15.01	91.0	79.8	355 + j 20	1.69

5. ψ = 20°

Frequency MHz	Max. Gain dBi	Front-Back Ratio dB	E BW degrees	H BW degrees	Impedance R +/- jX Ω	600-Ω SWR
50	8.79	6.11	73.8	56.8	776 + j 302	1.66
100	6.48	4.12	106.8	71.2	629 - j 56	1.11
150	7.44	5.23	98.8	55.2	693 + j 33	1.16
200	7.71	7.60	92.0	68.0	440 + j 95	1.43

As was the case with the trapezoidal LPA, the X version of the array shows increasing gain and decreasing front-to-back performance as we increase the ψ-angle. Also in concert with the trapezoidal version, the X array shows an approximate feedpoint resistance of about 600 Ω. The one exception to this rule is the flat version; here the impedance is closer to 500 Ω. The

entry for that version alone provides SWR values relative to both 600 Ω and 500 Ω. Notably, none of the 200-MHz SWR values exceeds 2:1, and the performance does not radically diminish at 200 MHz, as it did in the case of the trapezoidal LPA. Only the flat version of the array shows a noticeable decrease in forward gain at the highest frequency within the operating range.

The alternative way in which we may compare data both within the group of X LPAs and between the trapezoidal and X types is to summarize the sweep data from 50 to 200 MHz. The X LPA information appears in **Table 4**. There are three striking features within the table. First, the optimal ψ-angle is about 10°, if we use the criteria of the smallest change in gain and the smallest change in the E-plane beamwidth across the operating passband. We might have as easily selected the version in which ψ = 5°, since the overall rate of performance change with changes in the value of ψ is quite small. The selected ψ-angle angle is about half the value required by the trapezoidal array.

Table 4. Sweep data summary, 50-200 MHz in 5-MHz increments: X (saw tooth) array: 20 elements/bay, α = 17°, τ = 0.9

1. Ψ = 0° (flat array, 4" separation between bays)

Category	Minimum	Maximum	Δ	Average
Gain dBi	4.67	7.32	2.65	6.23
Front-Back dB	8.04	17.18	9.14	12.70
E Beamwidth °	74.2	116.4	42.2	91.0

2. ψ = 5°

Category	Minimum	Maximum	Δ	Average
Gain dBi	6.19	7.53	1.34*	6.87
Front-Back dB	9.79	18.26	8.47	15.10
E Beamwidth °	87.2	124.8	37.6	107.9

*Least variation across the passband of the group.

3. Ψ = 10°

Category	Minimum	Maximum	Δ	Average
Gain dBi	6.00	7.90	1.90	7.30
Front-Back dB	9.44	19.78	10.34	16.31
E Beamwidth °	73.0	107.6	34.6*	84.0

*Least variation across the passband of the group.

4. Ψ = 15°

Category	Minimum	Maximum	Δ	Average
Gain dBi	5.27	8.62	3.35	7.49
Front-Back dB	7.51	18.06	10.55	12.26
E Beamwidth °	65.6	134.2	68.6	86.5

5. ψ = 20°

Category	Minimum	Maximum	Δ	Average
Gain dBi	5.38	9.21	3.83	7.61
Front-Back dB	2.85	10.04	7.19	6.10
E Beamwidth °	45.6	158.2	112.6	88.8

In addition, the 10° ψ-angle also yields a very close coincidence between the E-plane and the H-plane beamwidths, as shown in the gallery of patterns in **Fig. 11**. Indeed, when ψ = 10°, we find a near symmetry in the patterns for the two planes. In general, the X array yields narrower beamwidths than the trapezoid.

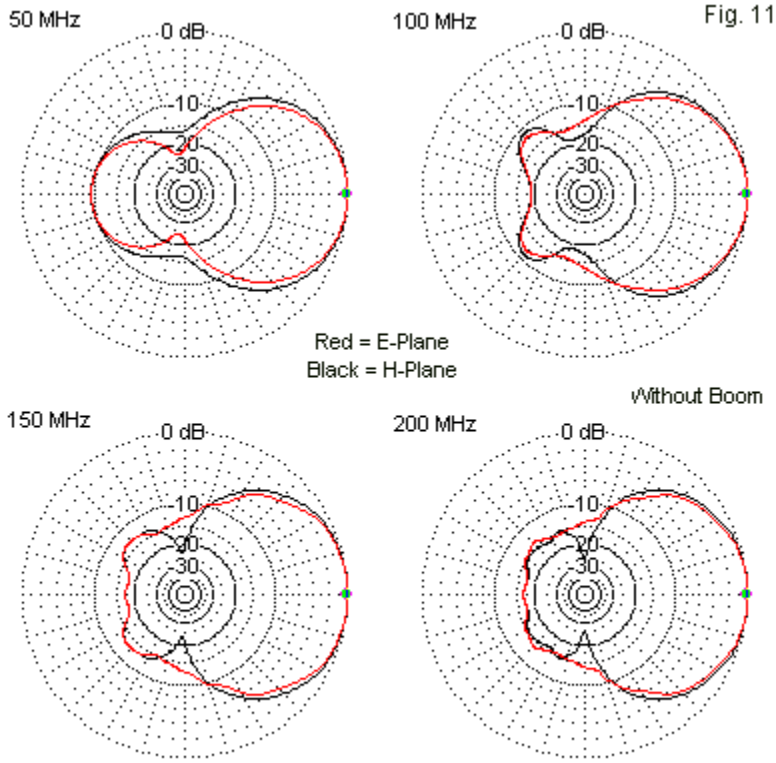

Fig. 11

Without Boom

20 Elements/Bay, Alpha = 17°, Tau = 0.9, Psi =10°
Sample Free-Space E-Plane and H-plane Patterns

Second, average gain across all versions of the boomless X array tends to be higher by an average of about 1 dB than the gain of the boomless trapezoidal LPA. Even with a ψ-angle of 0°, that is a flat array, the X LPA is capable of significant gain and a good front-to-back ratio, which goes some distance to explaining the popularity of the design in home-built TV antennas. The third notable factor is less debatable, since the range of change in both gain and the E-plane beamwidth is much smaller among the boomless X LPAs than among the trapezoidal counterparts. The general impression left by the X versions of the LPA is that they provide better pattern control across the operating bandwidth than do the trapezoidal arrays.

Fig. 13 and **Fig. 14** provide sweep graphs for the version of the array where ψ = 10°. Graphs for the other versions of the X LPA appear in the data appendix document. The sweep of forward gain and the 180° front-to-back ratio reveals that the design might benefit from a slightly longer rear element. We also saw this feature in the corresponding sweep for the trapezoidal array, but there, the effect was more pronounced at the low end of the operating range. At the upper end of the range, the gain and the front-to-back ratio show no significant decline, although the beamwidth tends to grow slowly with the operating frequency.

In common with the trapezoidal array, the X LPA SWR increases as the operating frequency exceeds about 185 MHz. However, the rate of increase is much smaller than we encountered with the trapezoidal array. Part of the reason for the slower rise in the 600-Ω SWR is the fact

that it is due to a declining feedpoint resistance, in contrast to the trapezoidal array that showed a rapid rise in the feedpoint resistance at the upper end of the passband.

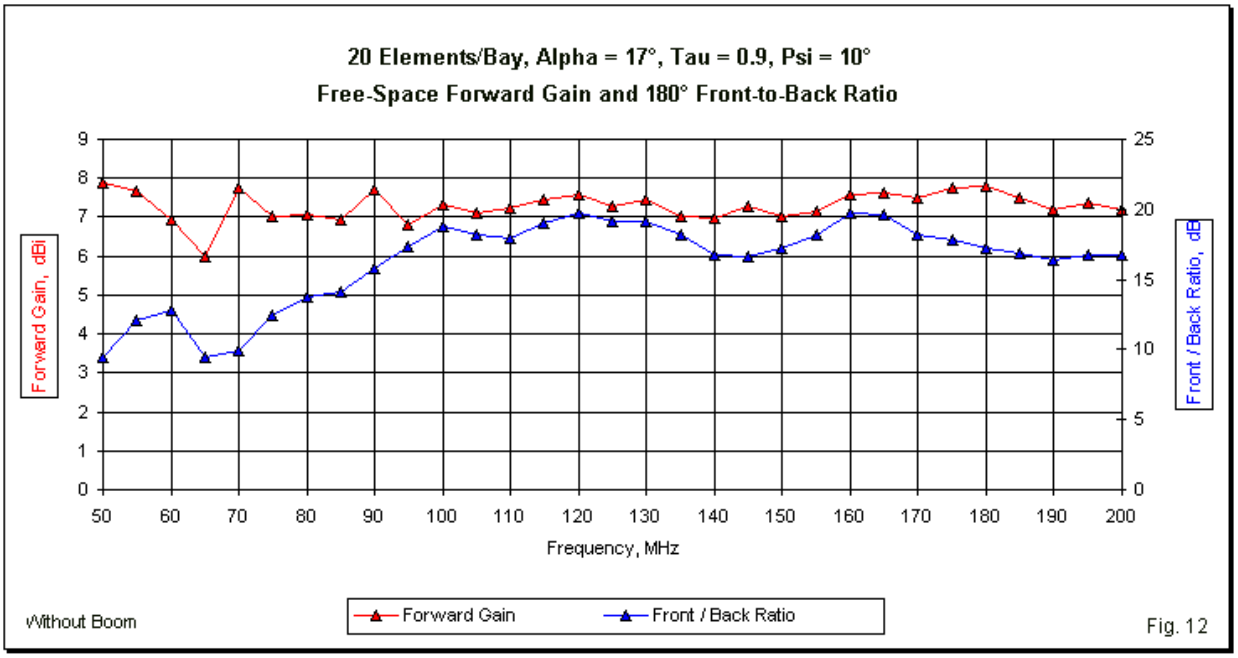

Fig. 12

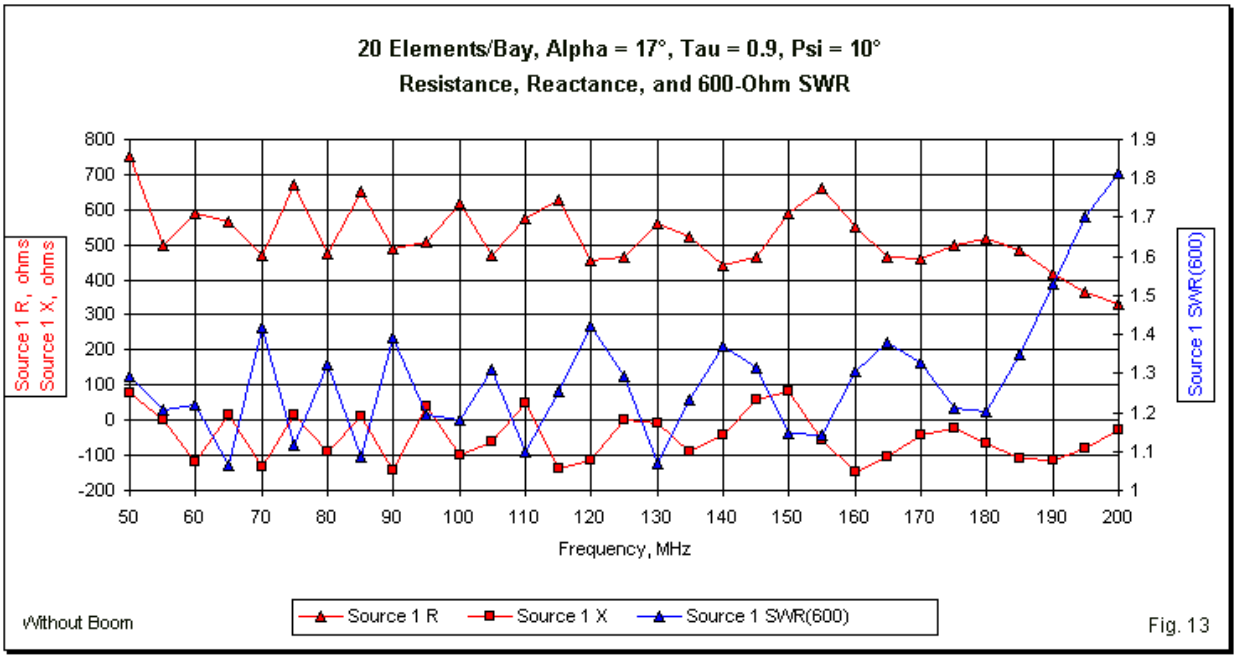

Fig. 13

The boomless X or saw tooth LPA leaves the impression that it is generally superior to the trapezoidal configuration in terms of performance at both ends of the operating passband and in terms of pattern control. The optimal configuration requires a smaller ψ-angle, and even a flat version is capable of reasonably good performance. The boomless X LPA still averages about a 2-dB gain deficit relative to either type of array when equipped with a boom and a 1-dB deficit relative to a single-bay LPDA. The boomless X LPA also has a somewhat lower front-to-back

average value than its boom-equipped counterpart. Still, if we measure simplicity of construction against the deficits in performance, the boomless X LPA yields an honest debate, whereas the boomless trapezoidal array performed too poorly to contemplate its use.

A Larger X LPA with Boom from Amateur Literature

Rothammels Antennenbuch contains not only a trapezoidal zig-zag array for potential home replication, but as well 2 X LPAs. Unfortunately, each array uses a different set of design parameters, so we can only sample their performance individually. **Fig. 14** shows the outline of the larger of two X LPAs with central booms. The array uses 12 elements, which suggest a higher value of τ (0.84). Like the trapezoidal array that we examined in Part 2, the values of α' and of ψ are 60° and 45°, respectively. Also like the trapezoidal array, the shortest elements are close enough to the vertex the permit extensions of the final element and the boom to that point.

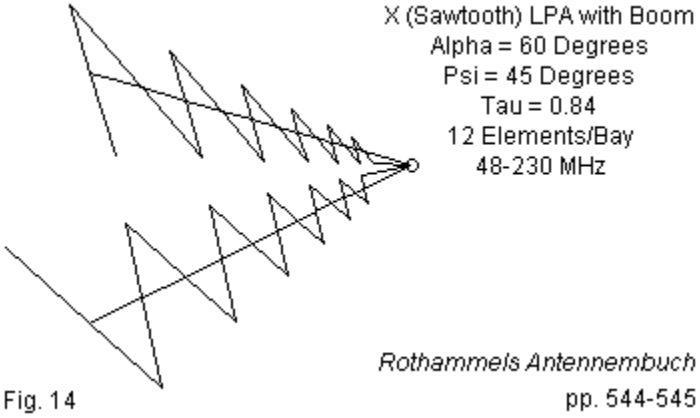

Fig. 14

The specified design range for the array was 48 to 230 MHz. However, calculations of the element locations appear to have used a minimum design frequency of 50 MHz. The dimensions appear in **Fig. 15** in a 2-part table. The lower section shows the calculation of the boom positions for the array. The models for this array used 2.54-mm (0.1") diameter lossless wire. **Table 5** samples the arrays performance at 50, 100, 150, and 200 MHz.

Table. 5. Sample performance values: 12 elements/bay, α = 60°, τ = 0.84, ψ = 45°

Frequency MHz	Max. Gain dBi	Front-Back Ratio dB	E BW degrees	H BW degrees	Impedance R +/- jX Ω	300-Ω SWR
50	5.64	3.09	72.9	92.2	375 – j458	3.64
100	8.49	11.88	67.8	74.0	294 + j 41	1.15
150	8.44	10.51	63.8	73.4	380 + j 0	1.27
200	8.69	11.50	63.2	74.6	225 - j 28	1.36

Although the trapezoidal amateur array that we looked at in Part 2 showed relatively smooth gain and front-to-back performance for the entire passband, the X LPA shows a serious deficit at the lowest sampled frequency. Moreover, the feedpoint impedance at this frequency shows a very high reactive component, raising the 300-Ω SWR value to uncomfortably high levels. Above the lowest frequency, the performance levels out at gain values only about 1 dB lower

than the X LPA using a τ of 0.9. However, the front-to-back values correspond only to those we might obtain from a 2-element driver-reflector Yagi.

Zig-Zag Log-Periodic Antenna Elements											Fig. 15
DARC Large X-LPA		p. 544									
Work Sheet		**Bold = User Entry**									
Tau		**0.840**								Sigma	0.069
Alpha	degrees	**60.00**	degrees	1.047	radians	1/2Alpha	0.524	tanAlpha	0.5774		0.069
F-low		**50.00**	MHz								
F-high		**200.00**	MHz								
L-long		3.00	meters	9.84	feet	118.11	inches				
Lhigh		0.75	meters	2.46	feet	29.53	inches				
L*1.6		0.47	meters	1.54	feet	18.45	inches				
Rv	Vertex R	2.60	meters	8.52	feet	102.29	inches				
Element	Ln	Ln/2	Rn	Element	Lfeet	Lft/2	Rfeet	Element	Linch	Lin/2	Rinch
1	3.000	1.500	2.598	*1*	9.84	4.92	8.52	*1*	118.11	59.06	102.29
2	2.520	1.260	2.182	*2*	8.27	4.13	7.16	*2*	99.21	49.61	85.92
3	2.117	1.058	1.833	*3*	6.94	3.47	6.01	*3*	83.34	41.67	72.17
4	1.778	0.889	1.540	*4*	5.83	2.92	5.05	*4*	70.00	35.00	60.63
5	1.494	0.747	1.294	*5*	4.90	2.45	4.24	*5*	58.80	29.40	50.93
6	1.255	0.627	1.087	*6*	4.12	2.06	3.56	*6*	49.40	24.70	42.78
7	1.054	0.527	0.913	*7*	3.46	1.73	2.99	*7*	41.49	20.75	35.93
8	0.885	0.443	0.767	*8*	2.90	1.45	2.52	*8*	34.85	17.43	30.18
9	0.744	0.372	0.644	*9*	2.44	1.22	2.11	*9*	29.28	14.64	25.35
10	0.625	0.312	0.541	*10*	2.05	1.02	1.77	*10*	24.59	12.30	21.30
11	0.525	0.262	0.454	*11*	1.72	0.86	1.49	*11*	20.66	10.33	17.89
12	0.441	0.220	0.382	*12*	1.45	0.72	1.25	*12*	17.35	8.68	15.03
13	0.370	0.185	0.321	*13*	1.21	0.61	1.05	*13*	14.58	7.29	12.62

X-LPA Boom Calculations			
Adjacent	2.76		
Opposite	0.415692		
tanBeta	0.150613		
Rbm-n	2.372157		
Boom	Rbm-m	Rbm-ft	Rbm-in
1-2	2.372	7.78	93.39
2-3	1.993	6.54	78.45
3-4	1.674	5.49	65.90
4-5	1.406	4.61	55.35
5-6	1.181	3.87	46.50
6-7	0.992	3.25	39.06
7-8	0.833	2.73	32.81
8-9	0.700	2.30	27.56
9-10	0.588	1.93	23.15
10-11	0.494	1.62	19.45
11-12	0.415	1.36	16.33
12-13	0.349	1.14	13.72

Table 6. Frequency sweep summary: 50-200 MHz: 8 elements/bay, α = 60°, τ = 0.84, ψ = 45°

Category	Minimum	Maximum	Δ	Average
Gain dBi	5.64	9.24	3.60	8.35
Front-Back dB	3.09	12.38	9.29	10.46
E Beamwidth °	59.1	74.4	15.3	67.5

The sweep summary in **Table 6** reveals the same set of impressions. Still, among arrays with high values of ψ and α', the array does show relatively smooth E-plane patterns without too much variation in the beam width. However, as **Fig. 16** makes clear, the array exhibits less control over the rearward lobe structure. In terms of 1970-era television reception, the antenna would be subject to interference from distant stations anywhere within the rearward quadrants.

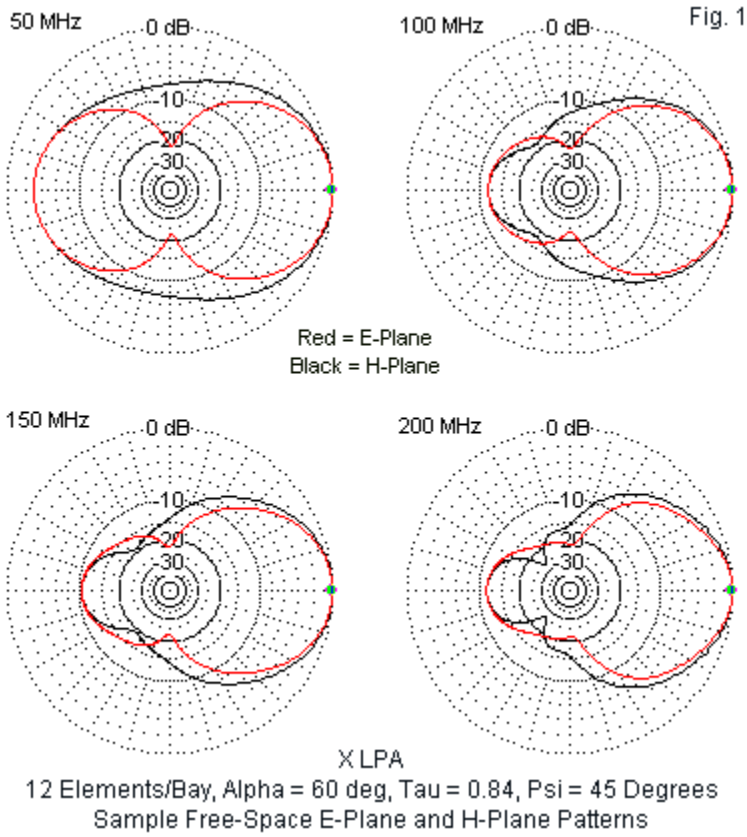

Fig. 16

X LPA
12 Elements/Bay, Alpha = 60 deg, Tau = 0.84, Psi = 45 Degrees
Sample Free-Space E-Plane and H-Plane Patterns

The sweep graphs in **Fig. 17** and **Fig. 18** confirm the tabular information. Note that the performance drop near the lower end of the passband begins at a higher frequency than the impedance deficit, a property that we have seen in other X LPAs.

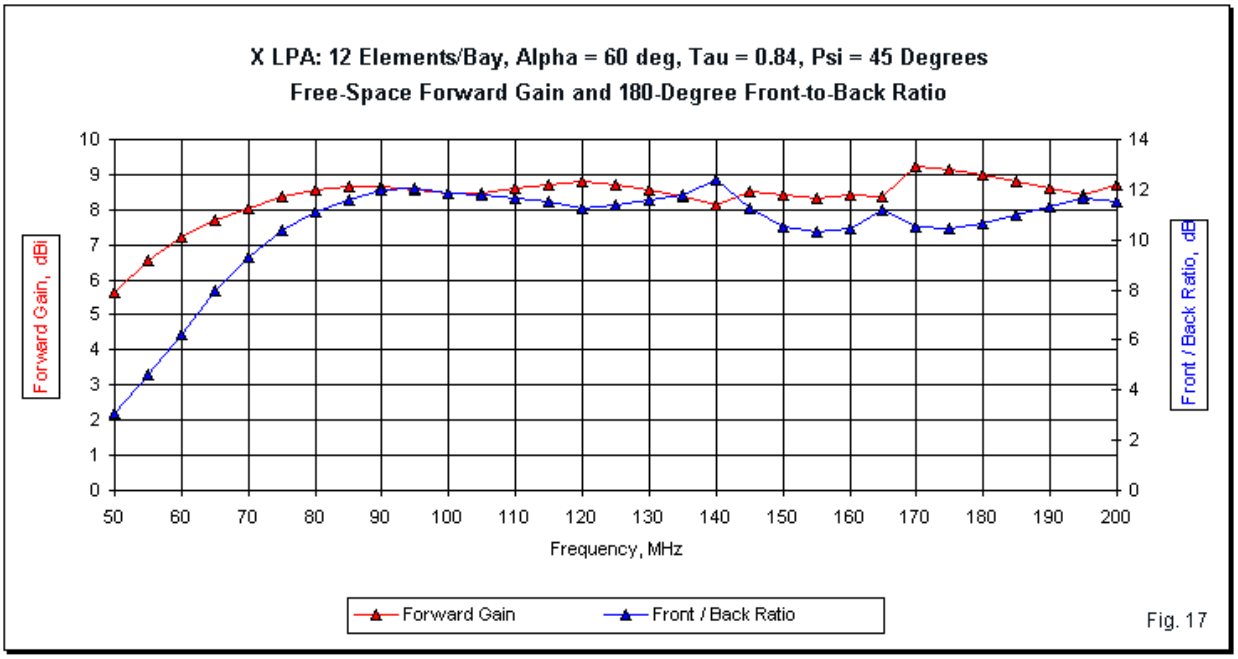

Fig. 17

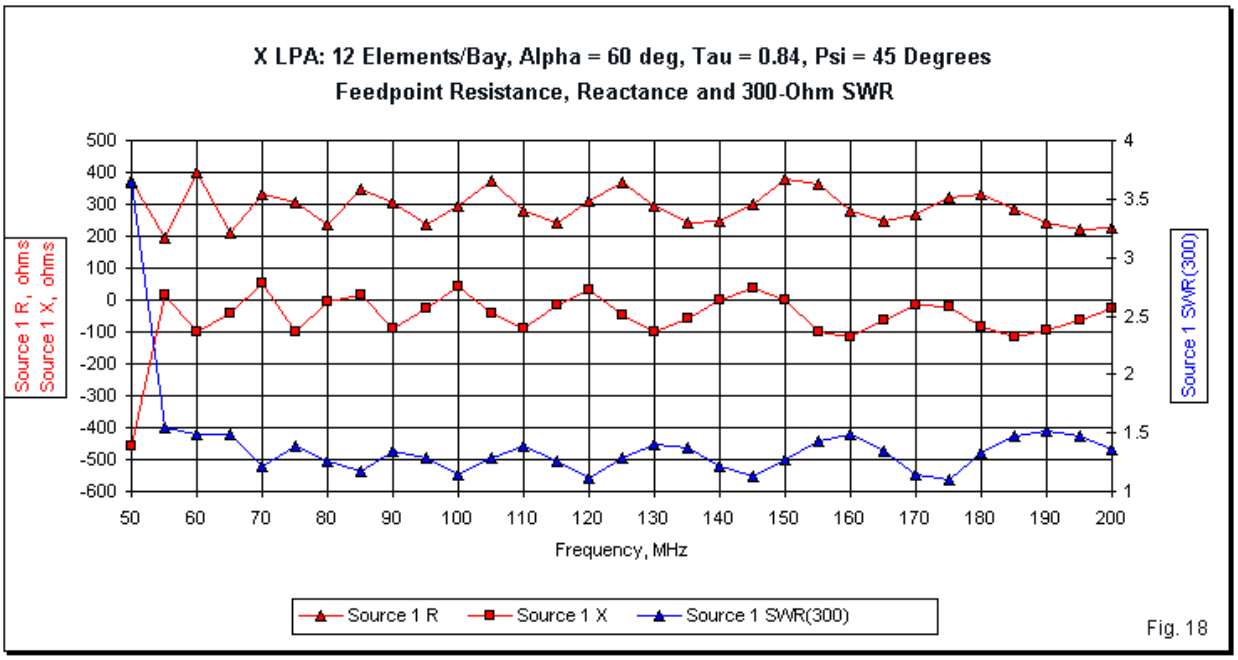

A Smaller X LPA with Boom from Amateur Literature

Rothamel also presents a smaller X LPA that uses only 8 elements, with a τ of 0.707. The ψ-angle remains a standard 45°. The listed value of α' was 75°, but I had to reduce the angle to 70° to bring the listed dimensions into coincidence with standard calculations of element dimensions. **Fig. 19** shows the outline of the array.

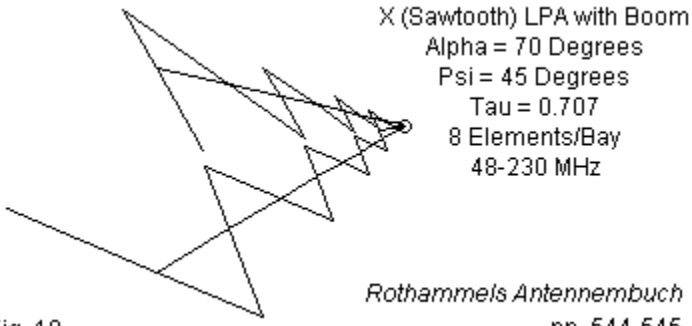

The dimensions used in the model appear in **Fig. 20**, which again has an upper and a lower section. The lower portion shows the relevant boom calculations. Like the larger X LPA, the smaller version draws the end of the shortest element and the boom all the way to the vertex. The distance is fairly short, as indicated by the smallest value of Rn in the dimension table.

Table 7 and **Table 8** present the performance sampling information and the sweep data summary, respectively. The performance deficiencies at the low end of the passband once more stand out in both tables. The one interesting category is the 200-Ω SWR value set. The small array manages to maintain values that are less than 2:1 at all sampled frequencies. Once more, the X LPA impedance performance has broader-banded characteristics than the gain, although the SWR does rise a small amount above 2:1 at 2 points in the passband.

Zig-Zag Log-Periodic Antenna Elements											Fig. 20
DARC X-LPA-Small			p. 544								
Work Sheet		**Bold = User Entry**									
Tau		**0.707**								Sigma	0.105
Alpha	degrees	**70.00**	degrees	1.222	radians	1/2Alpha	0.611	tanAlpha	0.7002		0.105
F-low		**48.00**	MHz								
F-high		**230.00**	MHz								
L-long		3.13	meters	10.25	feet	123.03	inches				
Lhigh		0.65	meters	2.14	feet	25.68	inches				
L*1.6		0.41	meters	1.34	feet	16.05	inches				
Rv	Vertex R	2.23	meters	7.32	feet	87.85	inches				
Element	Ln	Ln/2	Rn	Element	Lfeet	Lft/2	Rfeet	Element	Linch	Lin/2	Rinch
1	3.125	1.563	2.231	*1*	10.25	5.13	7.32	*1*	123.03	61.52	87.85
2	2.209	1.105	1.578	*2*	7.25	3.62	5.18	*2*	86.98	43.49	62.11
3	1.562	0.781	1.115	*3*	5.12	2.56	3.66	*3*	61.50	30.75	43.91
4	1.104	0.552	0.789	*4*	3.62	1.81	2.59	*4*	43.48	21.74	31.05
5	0.781	0.390	0.558	*5*	2.56	1.28	1.83	*5*	30.74	15.37	21.95
6	0.552	0.276	0.394	*6*	1.81	0.91	1.29	*6*	21.73	10.87	15.52
7	0.390	0.195	0.279	*7*	1.28	0.64	0.91	*7*	15.37	7.68	10.97
8	0.276	0.138	0.197	*8*	0.91	0.45	0.65	*8*	10.86	5.43	7.76
9	0.195	0.098	0.139	*9*	0.64	0.32	0.46	*9*	7.68	3.84	5.48

X-LPA Boom Calculations			
Adjacent	2.667188		
Opposite	0.653824		
tanBeta	0.245136		
Rbm-n	1.848456		
Boom	Rbm-m	Rbm-ft	Rbm-in
1-2	1.848	6.06	72.77
2-3	1.307	4.29	51.45
3-4	0.924	3.03	36.38
4-5	0.653	2.14	25.72
5-6	0.462	1.52	18.18
6-7	0.327	1.07	12.86
7-8	0.231	0.76	9.09
8-9	0.163	0.54	6.43

Table. 7. Sample performance values: 8 elements/bay, α = 70°, τ = 0.707, ψ = 45°

Frequency MHz	Max. Gain dBi	Front-Back Ratio dB	E BW degrees	H BW degrees	Impedance R +/- jX Ω	200-Ω SWR
50	4.09	1.75	75.7	134.0	203 – j112	1.73
100	6.96	10.73	66.8	89.6	223 + j 7	1.12
150	6.32	9.90	80.8	105.8	260 + j 28	1.33
200	6.92	9.67	79.4	99.6	209 - j 38	1.21

Table 8. Frequency sweep summary: 50-200 MHz: 8 elements/bay, α = 70°, τ = 0.707, ψ = 45°

Category	Minimum	Maximum	Δ	Average
Gain dBi	4.09	7.20	3.11	6.37
Front-Back dB	1.75	12.45	10.70	8.69
E Beamwidth °	64.0	80.8	16.8	70.9

As we might expect from such a sparsely populated array, pattern control decays more significantly than we found in the larger amateur X LPA. As shown in **Fig. 21**, the rearward lobes of the array at all sampled frequencies allow for considerable interference from the rear. The E-plane beamwidth values are close to those that are typical of a simple dipole.

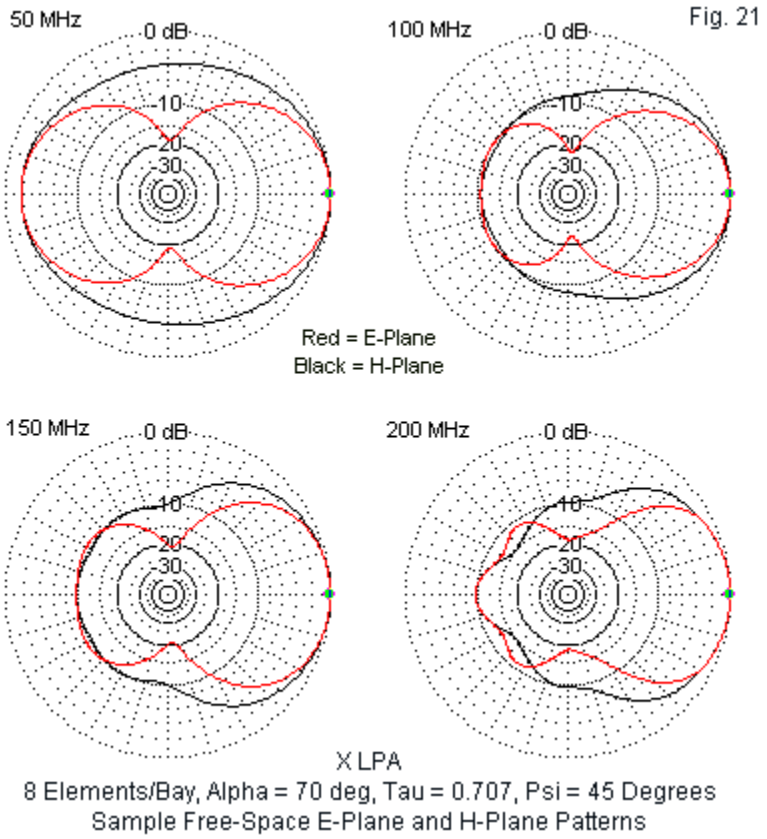

Fig. 21

Fig. 22 and **Fig. 23** provide sweep graphs that correlate with the tabular information. The gain and front-to-back graph is notable for two reasons. First, the performance curves are subject to sudden changes. Second, the low-end performance deficiencies cover a wider portion of the total passband.

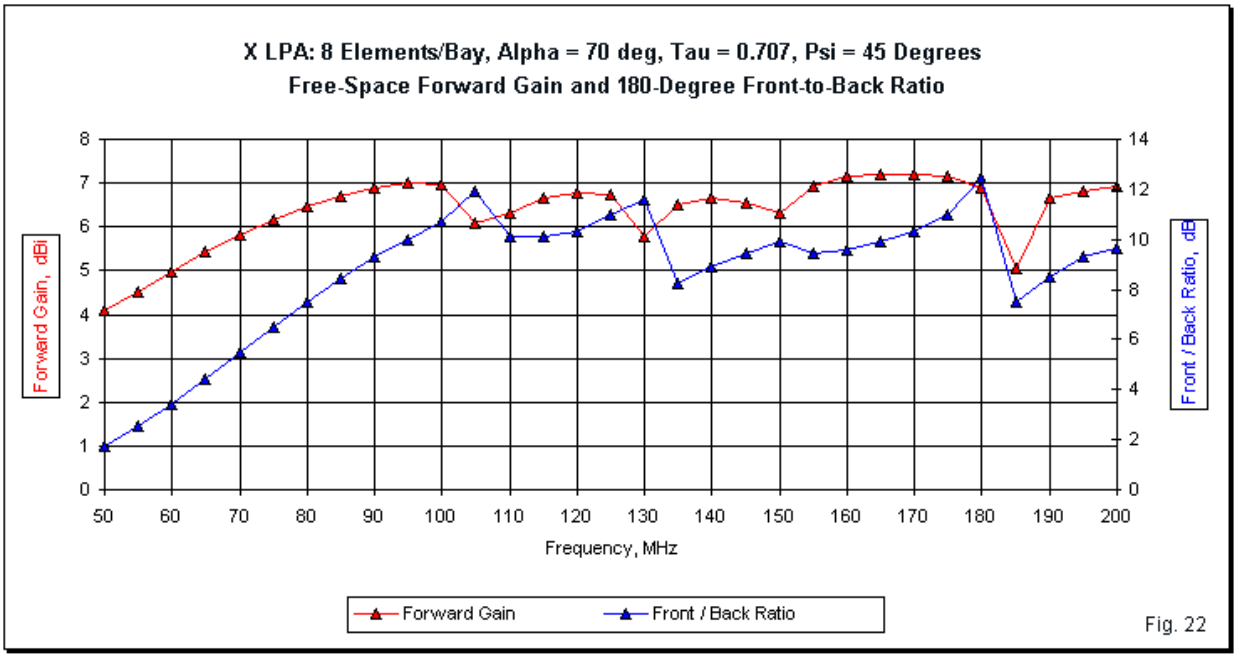

Fig. 22

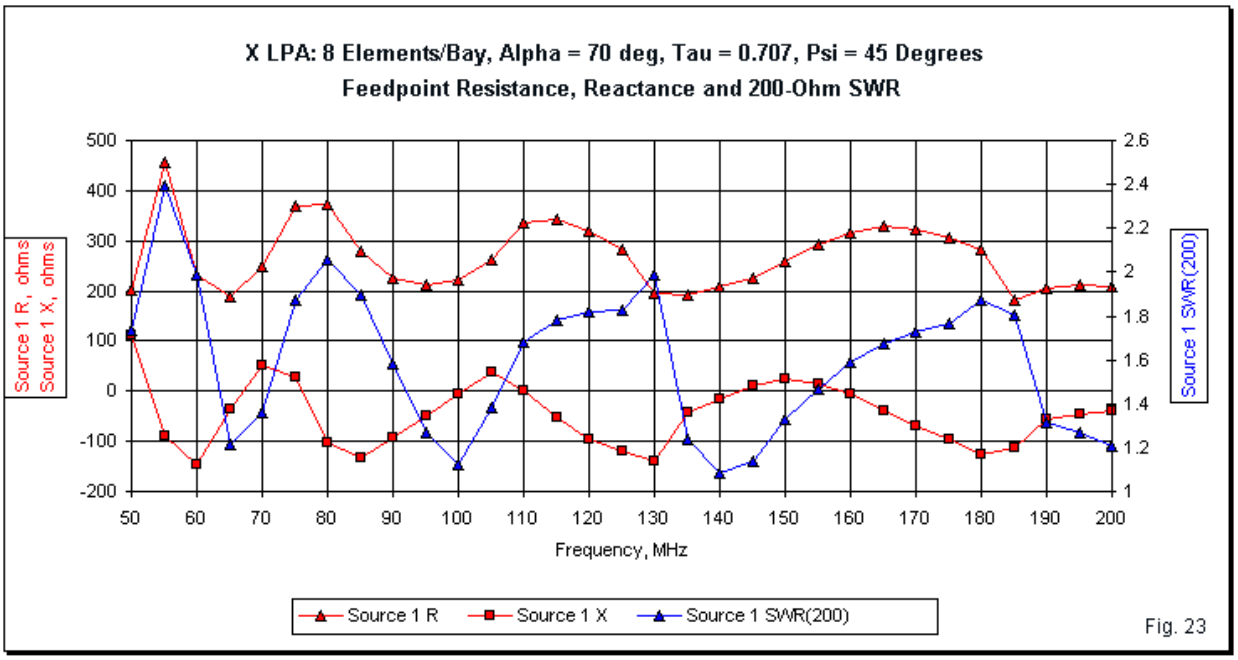

The impedance graph reveals that the small X LPA undergoes more radical changes in both resistance and reactance than the larger array. As well, we can easily find the SWR excursions above 2:1 at 55 and 80 MHz, with a borderline case at 130 MHz.

Of the two old-style X LPA designs, only the larger version might pass muster for adequate wide-band performance by 21st century standards—and then, only if we correct the deficiencies at the lower end of the passband. While we make those corrections, we might also experiment with the optimum value for the ψ-angle and not blithely accept the 45° standard that was common when these designs emerged.

Conclusion

Our main goal in all three parts of this exercise has been to compare the performance of "standard" LPDA design against zig-zag LPA designs that came earlier. To level of field of comparison, we used a fixed set of design parameters for all of our candidate designs: $\tau = 0.9$, $\sigma = 0.167$, $\alpha' = 17°$. All arrays used 20 0.1"-diameter elements per bay. Since the zig-zag designs required experimental selection of the ψ-angle, we let that factor be a variable.

Virtually none of the configurations showed exceptionless performance across the entire passband, a condition that we created by limiting the compensatory steps normally used to define the operative dimensions. Some versions showed weakness at the low end of the operating range, while others saw declines nearer to the upper end. Virtually all of the designs (with the exception of the boomless trapezoidal array) are subject to relatively easy reworking to correct the deficiencies, but the result will be as many different designs as we have types of LPAs.

Along the way, we have made some relevant comparisons between and among configurations. Repeating those textual assertions might leave their foundations uncertain. Therefore, by way of final summary, I have created **Table 9**, a compilation of the sweep summaries of the representative arrays of all types covered in these notes. The data allow you

to draw your own conclusions. For further data on variations of each LPA type, see the data appendix.

Table 9. Sweep data summary, 50-200 MHz in 5-MHz increments

LPDA, single-bay

Category	Minimum	Maximum	Δ	Average
Gain dBi	7.33	8.52	1.19	8.09
Front-Back dB	16.71	44.56	27.85	28.93
E Beamwidth °	60.8	66.4	5.6	63.7

Double-bay, Ψ=10°

Category	Minimum	Maximum	Δ	Average
Gain dBi	9.35	10.79	1.18	10.00
Front-Back dB	14.28	63.75	49.47	35.93
E Beamwidth °	54.0	61.0	7.0	57.8

Trapezoidal zig-zag LPA, with boom, ψ = 5°

Category	Minimum	Maximum	Δ	Average
Gain dBi	7.71	8.57	0.86	8.35
Front-Back dB	20.13	32.04	11.91	27.12
E Beamwidth °	63.0	68.8	5.8	65.0

Trapezoidal zig-zag LPA, without boom, Ψ = 20°

Category	Minimum	Maximum	Δ	Average
Gain dBi	4.48	8.20	3.72	6.57
Front-Back dB	4.46	13.60	9.14	9.94
E Beamwidth °	73.6	170.0	96.4	109.7

X zig-zag LPA, with boom, ψ = 5°

Category	Minimum	Maximum	Δ	Average
Gain dBi	7.64	8.84	1.20	8.64
Front-Back dB	11.96	30.93	18.97	26.87
E Beamwidth °	62.4	64.6	2.2*	63.5

X zig-zag LPA, without boom, ψ =10°

Category	Minimum	Maximum	Δ	Average
Gain dBi	6.00	7.90	1.90	7.30
Front-Back dB	9.44	19.78	10.34	16.31
E Beamwidth °	73.0	107.6	34.6	84.0